Progress In Electromagnetics Research C, Vol. 72, 187–196, 2017

A Novel Reconfigurable Antenna with Spectrum Sensing Mechanism for CR System

Sonia Sharma* **and Chandra C. Tripathi**

Abstract—A novel hybrid antenna capable of both spectrum sensing and then accordingly reconfiguring its operating characteristics is proposed here. The proposed antenna is versatile in nature as it can reconfigure its resonant frequency, polarization state, bandwidth and radiation pattern. The physical structure of antenna is also versatile in nature as different printed parts are used several times in different operating modes using PIN diodes. The proposed versatile antenna senses spectrum over a wide frequency range from 3 GHz–12 GHz by using a separate UWB antenna. After sensing, the antenna can reconfigure its frequency in five different bands using three matching stubs. The proposed antenna can reconfigure its polarization state over two frequency bands by controlling the switchable slot. The antenna can also reconfigure its pattern by shorting the parasitic arc using PIN diodes. The prototype is fabricated, and the functioning is verified through measurement.

1. INTRODUCTION

With the explosion of various wireless communication technologies, only Cognitive Radio (CR) has the potential to improve the future spectrum implications [1–4]. CR system identifies the spectrum condition at a specific time and smartly reconfigures the operating parameter of the system to increase the spectrum utility. Basically, CR system is integrated with two types of antenna: UWB antenna as a spectrum sensor and reconfigurable antenna for multiple communication purposes [1–4]. These two antennas are integrated together on a single substrate so that they work simultaneously without interfering with each others' characteristics. In literature, a separate UWB antenna is used as sensing antenna, and then reconfigurable antenna changes its characteristics by mechanical [5], optical [6, 7] or electrical [8–13] means. These antenna designs can smartly sense the spectrum and accordingly reconfigure either its frequency state or radiation pattern. However, single reconfigurable feature is not sufficient for today's wireless communication especially for CR. Multiple reconfigurable functionalities provide users with options of connecting to different kinds of wireless services at different times. In the available literature, there is not a single antenna that reconfigures its resonant frequency, polarization state, bandwidth and radiation pattern to meet the essential characteristics of CR.

So, in this paper, an antenna solution is presented which can reconfigure all its characteristics simultaneously in a single structure, hence, is versatile in nature. The proposed antenna is flexible and compact in nature, and there is the best utilization of printed circuits multiple times in different operating modes. Physical structure of the proposed antenna is also versatile in nature as each part is not bound to be used in single operating mode but is also actively used many times in other operating modes. PIN diodes are placed in such a position that the electrical switching of the PIN diodes makes every part of antenna multipurpose. Fig. 1 shows the layout of the proposed antenna in which a semi-circular 2D disk (right part) is used for sensing. The circular patch is used for frequency and polarization

Received 9 January 2017, Accepted 17 March 2017, Scheduled 31 March 2017

* Corresponding author: Sonia Sharma (sonia990@gmail.com).

The authors are with the Department of Electronics and Communication Engineering, UIET, Kurukshetra University, Kurukshetra, India.

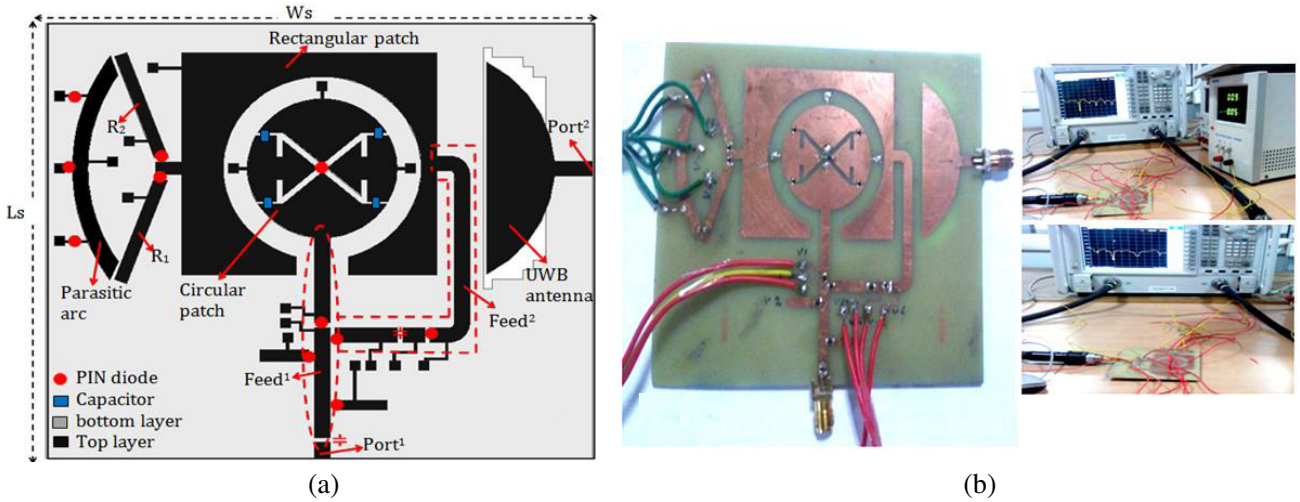

Figure 1. (a) Layout for proposed versatile antenna. (b) Fabricated prototype and experimental setup.

reconfiguration, and the rectangular patch is used for pattern reconfiguration and so on. The complete design evolution steps to insert the said objective of multiple reconfigurable features in the proposed antenna are explained in the next section.

2. DESIGN EVOLUTION

The proposed antenna can sense the spectrum using a separate UWB antenna to fulfill the condition of cognitive capability for CR system, but it requires more space. However, it adds to the versatility of the antenna solution since the two antennas can be designed separately. UWB antenna is a semi-circular 2D dish type structure which is excited by a microstrip feed-line via port^2 as shown in Fig. 2. To ensure the wideband response, a rectangular slot ($L_{r1} * W_{r1} = 10\,\text{mm} * 38\,\text{mm}$) is etched in the ground plane. To optimize the UWB response of antenna, the size of rectangular slot is varied, and its effect on S_{11} parameter is studied. Fig. 3(a) shows its effect on S_{11} characteristics, when length (L_{r1}) of the rectangular slot is varied from 8 mm to 15 mm. It is observed that when length (L_{r1}) is = 12 mm, the best UWB response is obtained from 3 to 10 GHz. But the simulated value of S_{11} is still very close to 10 dB in the entire UWB range, so there will be some probability that value of S_{11} degrades during the measurement.

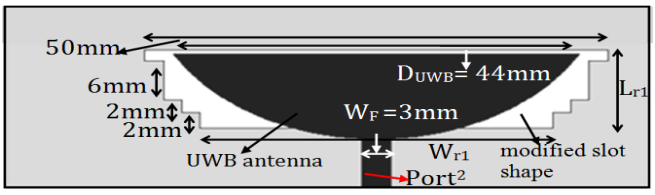

Figure 2. Active area of UWB antenna.

It is better to improve S_{11} initially in the simulation to reduce the measurement error. Therefore, to optimize the UWB behavior, the shape of therectangular slot is modified in the next design step. The optimized dimensions of modified staircase-shaped slot structure are shown in Fig. 2, and the comparison of S_{11} characteristics is shown in Fig. 3(b). Now, S_{11} is better than 15 dB in a wideband from 2 to 12 GHz.

The design steps considered for reconfigurable antenna are explained. The complete design strategy described here is not given in a sequential manner; rather major design steps for all operating modes

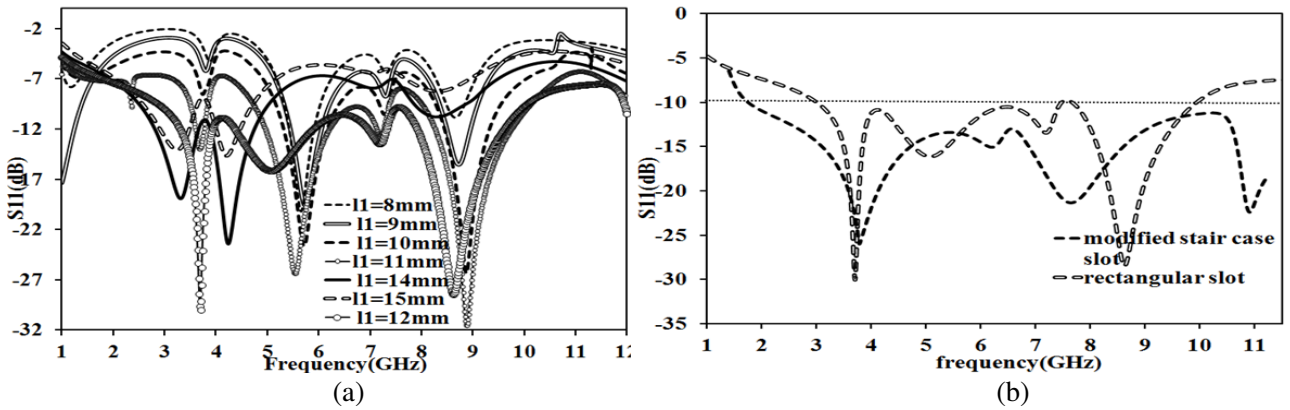

Figure 3. Effect on S_{11} for UWB antenna by (a) varying the length of rectangular slot, (b) modifying slot geometry.

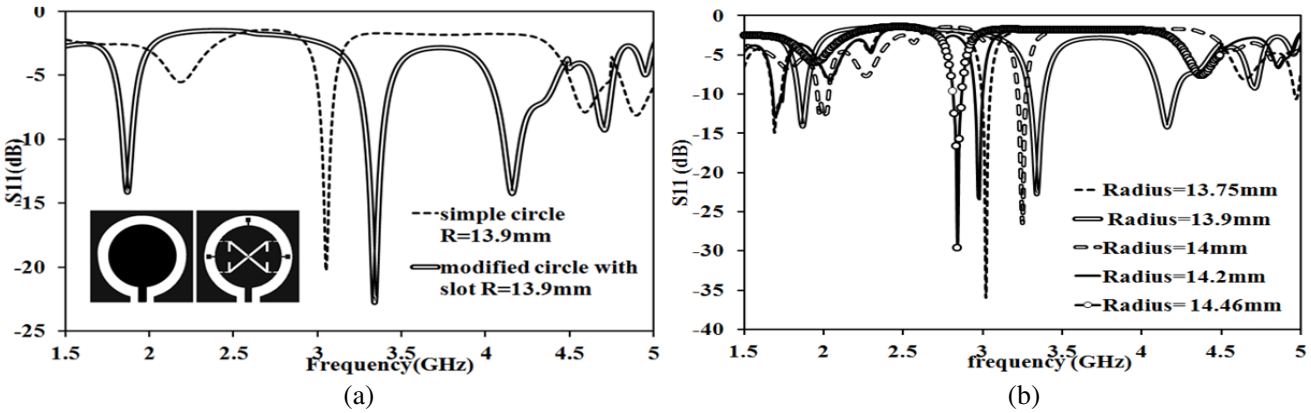

Figure 4. Comparison of S_{11} parameter by (a) inserting cross shape slot in circular patch, (b) varying radius.

are presented, because fixing or optimizing the dimension or parameter in one operating mode changes the performance (frequency and S_{11}) of antenna for other operating modes. So, the antenna needs to be completely re-optimized after each incremental design step. In this regard, design optimization of some steps is explained here to show the effect of dimensions on antenna performance. At first, a circular patch antenna is designed with radius = 13.9 mm for 3 GHz. Fig. 4 shows S_{11} vs. frequency for a simple circular patch. In the next design step, a rectangular patch which completely encloses the circular patch is designed and optimized. These two independent antennas require minimum space for their integration as circular patch is embedded inside the empty space of the rectangular antenna. In the next step, cross-shape slots are etched in the circular patch to switch the polarization state. The dimensions and shape of slots are finalized by optimizing the value of RL and axial ratio at center frequency after the placement of bias lines, DC pads, equivalent circuit for diode and SMD capacitor, etc. After adding modified cross-shape slots, geometry of circular patch is modified which results in the shift of resonant frequency to 3.4 GHz. Moreover, S_{11} parameter of circular antenna is disturbed due to the presence of slot, slits and biasing network as shown in Fig. 4(a). So, dimension optimization should be done, to tune the resonant frequency of circular antenna to nullify the effect of other elements. The effect of variation in radius size is shown in Fig. 4(b), and it is found that S_{11} of the antenna is improved when radius of the circle is increased from 13.75 to 14.46 mm.

Now to achieve the frequency reconfiguration in the circular antenna, microstrip open stubs are placed at proper positions, so that these stubs match the antenna's input impedance at different frequencies. To optimize the antenna for desirable and independent frequency controls, effect of stub

length on the scattering parameter has been studied after placing bias lines, DC pads, etc. Dimension of stub[1] is selected after analyzing the result as shown in Fig. 5(a). Similarly, optimization of stub[2] dimensions is done to get the optimally tuned frequency for stub[2] without affecting the resonating frequency for stub[1] as shown in Fig. 5(b). Finally, the matching at the third resonant frequency is done by placing stub[3] in the feed line, and optimization is done using parametric study as shown in Fig. 5(c). The final selection of dimension for all stubs from parametric study is taken by considering various factors such as dimensional constraint, unwanted non-resonant sidebands, RL value at desired frequency, and amount of nonlinearity present in the frequency response. Geometrical parameters of

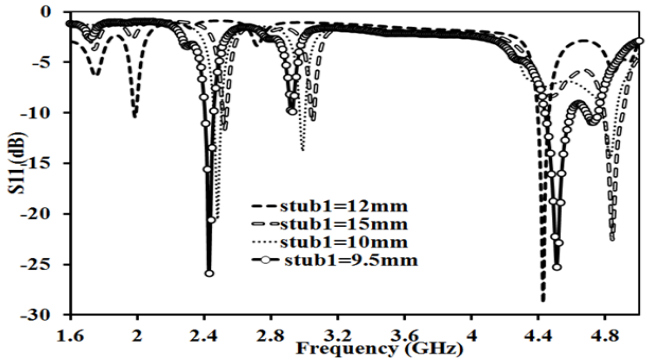

(a)

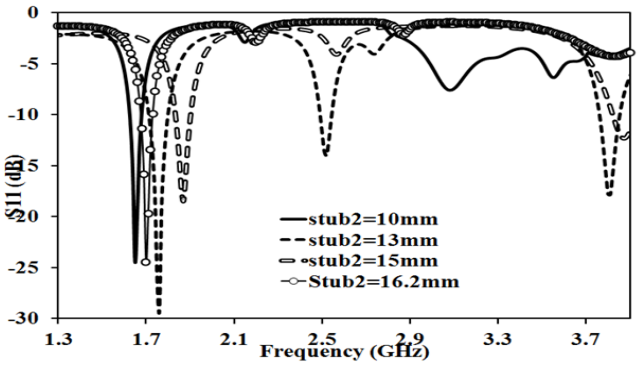

(b)

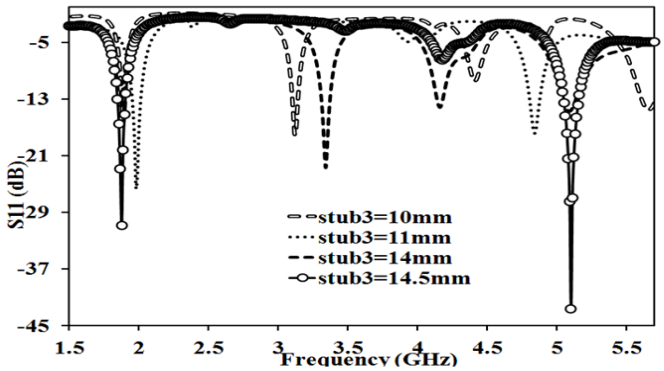

(c)

Table 1 Geometry Dimensions for proposed antenna (mm)

Substrate L_s, W_s	Stub[1] L_1,W_1	Stub[2] L_2,W_2	Stub[3] L_3,W_3
85, 85	9.5, 3	16.2, 2	14.5, 3
Rect. patch L_R,W_R	Circular patch Radius	F_1	F_2
45.5, 49	14.46	27	17.67

Figure 5. Effect on S_{11} parameter by changing the length of (a) stub[1], (b) stub[2], (c) stub[3].

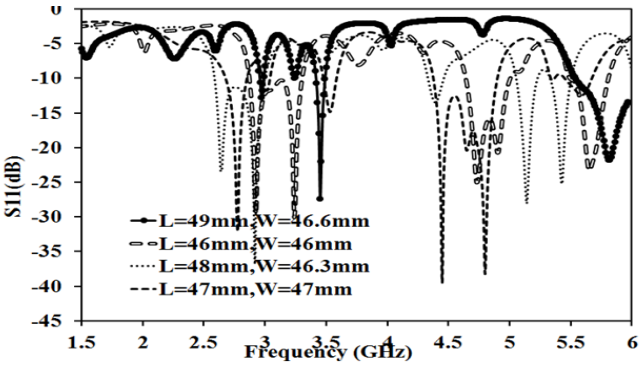

(a)

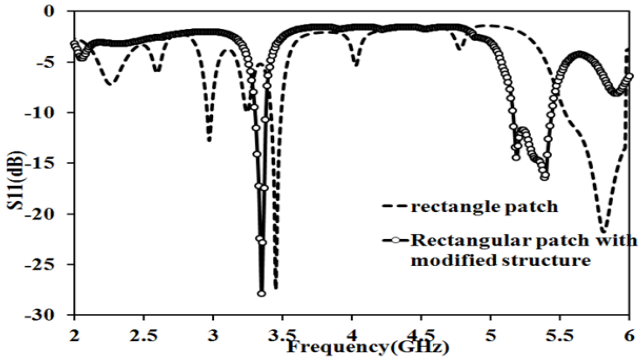

(b)

Figure 6. Effect on S_{11} parameter (a) varying length and width of rectangular patch, (b) by modifying structure.

the proposed antenna are given in Table 1. The designed circular patch is used in two operating modes. When the stubs placed across the feed line are controlled electronically, the circular antenna is used in frequency reconfiguration mode. The same circular patch is used in polarization reconfiguration mode when diodes placed inside the modified cross-shaped slots are controlled. The feeding structure of antenna is used to feed both circular and rectangular patch antennas independently by splitting itself into two parts using PIN diodes. For pattern reconfiguration mode, the main input signal is used to excite the rectangular antenna instead of circular antenna. The dimensions of the rectangular antenna are optimized for the fine tuning of resonant frequency. Fig. 6(a) shows the effect of variation in length and width of the rectangular patch on S_{11} parameter. The final optimized dimensions are $L_R = 49$ mm, $W_R = 46.6$ mm which make the antenna resonate efficiently at 3.5 GHz. This rectangular patch is used for pattern and frequency reconfiguration mode. In the next design step, two rectangular bars R_1 and R_2, and a parasitic arc are attached with the rectangular antenna for pattern reconfiguration mode. The dimensions of these two rectangular bars which are 120° apart from each other are so chosen that they do not disturb the resonant frequency of rectangular patch as shown in Fig. 6(b). The complete geometry description for pattern reconfiguration is explained in the next section.

3. WORKING OPERATION AND IMPLEMENTATION

To validate the proposed design, the prototype is fabricated, and results are verified experimentally. A step-by-step design strategy and functioning for achieving the desired objectives in a single antenna are explained below:

3.1. Frequency Reconfigurabilty Mode

Figure 7(a) shows the active portion of hybrid antenna when being operated in frequency reconfigurable mode. Black color shows the active portion as it is directly attached to the RF port, and grey portion shows the passive portion as no RF signal is applied to it. The heart of the proposed design is electronically switchable feeding structure which is specially designed for this mode. Five PIN diodes are used to control the activation of different stubs independently. The diode positioning and DC biasing scheme are given in Fig. 7(b). Complete feeding structure is composed of 3 feed lines (F_1, F_2, F_3); 3 micro strips open stubs (S_1, S_2, S_3), 5 PIN Diodes (D_1, D_2, D_3, D_4, D_5), 2 SMD capacitor (C_1, C_2) and DC voltage pads (V_1, V_2, V_3, V_4, V_{1-}). Operating states of PIN diodes are changed by providing DC voltage on their respective DC pad. The orientations of PIN diodes are such that they share single ground pad (V_{1-}). The SMD capacitor C_1 is placed in the main feed line section F_1 to provide DC isolation towards RF port. The SMD capacitor C_2 is placed in the stub[3], to bias the diode D_4 and D_5 independently. The circular patch is selected by forward biasing the diode D_1 to activate

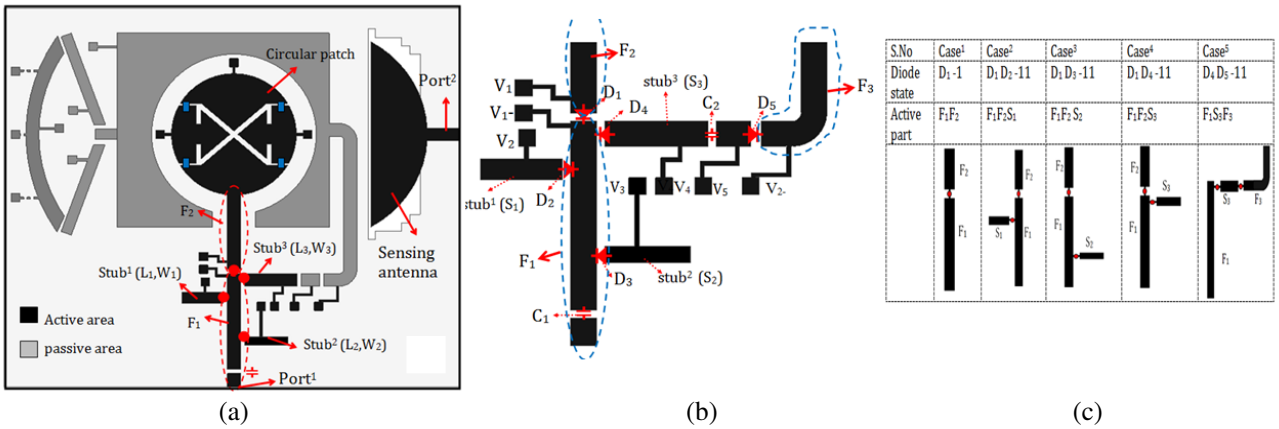

Figure 7. (a) Active portion of antenna in frequency reconfiguration mode, (b) biasing circuitry for PIN diodes, (c) pictorial view for different case studied.

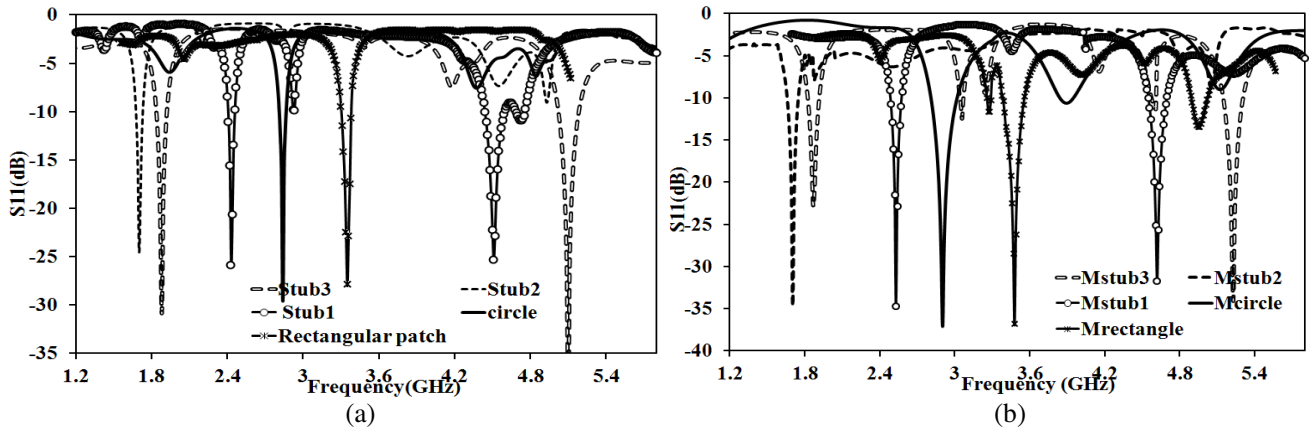

Figure 8. S_{11} vs. frequency for frequency reconfiguration mode. (a) Simulated. (b) Measured.

the feed portion F_1F_2, and the rectangular patch is selected by forward biasing the diode D_4 and D_5 to activate feed portion $F_1S_3F_3$. The combination of feed line structure F_1F_2 is named as Feed^1, and the combination of $F_1S_3F_3$ is named as Feed^2. Different cases are discussed using different combinations of PIN diodes to select different portions of the antenna. Fig. 7(c) describes the different cases studied in this mode along with their diode conditions and pictorial views of active feed part.

For frequency reconfiguration mode, main circular patch is exited by feed^1, and frequency tuning is done by activating different stubs electronically through PIN diodes. Diode D_1 is always ON in this case, and four different cases are discussed using different combinations of PIN diodes as shown in Fig. 7(c). The simulated and measured S_{11} vs. frequency are shown in Figs. 8(a)–(b). In case^1, when diode D_1 is forward biased by applying +5 V on DC pad $+V_1$, feed line structure F_1F_2 (feed^1) is selected which excites the main circular patch. In this case, simulated resonant frequency is 2.84 GHz with RL = 30 dB whereas measured frequency is found at 2.85 GHz with RL = 38 dB. In case^2, when diode D_1 and D_2 are forward biased, feed^1 is selected in conjunction with stub^1 ($F_1F_2S_1$ configuration) to tune the antenna at another frequency. In this case, simulated dual bands are obtained at 2.4 GHz and 4.5 GHz with RL = 28 dB and 27 dB, respectively, whereas measured dual bands are obtained at 2.5 GHz and 4.7 GHz with RL = 35 dB and 32 dB, respectively. For case^3, when diodes D_1 and D_3 are forward biased, feed^1 is selected along with stub^2 ($F_1F_2S_2$) to switch the antenna frequency. In this case, simulated resonant frequency is 1.7 GHz with RL = 25 dB whereas measured resonant frequency is 1.73 Hz with RL = 35 dB. In case^4, when diode D_4 is forward biased, feed^1 is selected along with stub^3 ($F_1F_2S_3$) to tune the antenna frequency. In this case, simulated dual bands are obtained at 1.85 GHz and 5.1 GHz with RL = 30 dB and 36 dB, respectively, whereas measured dual bands are obtained at 1.88 GHz and 5.23 GHz with RL = 24 dB and 35 dB, respectively. In case^5, the feed^2 is selected by forward biasing the diodes D_4 and D_5 to feed the rectangular antenna. The simulated resonant frequency is 3.5 GHz with RL = 29 dB whereas measured resonant frequency is 3.52 GHz with RL = 38 dB.

3.2. Polarization Reconfiguration Mode

Figure 9(a) shows the active part of hybrid antenna when being operated in polarization reconfiguration mode. To change the polarization state, PIN diodes D_6 and D_7 are controlled electronically, which are placed inside the modified cross-shaped slot. The dimensions of modified cross-shaped slots are $l_1 = 9.713$ mm, $l_2 = 4.5$ mm. Four thin slits of 0.2 mm wide are etched in the circular patch and divide the patch into four regions R_1, R_2, R_3, and R_4 as shown in Fig. 9(b). Placing 4 SMD capacitors over these slits makes the RF continuity among the four regions (R_1, R_2, R_3, R_4). Now these regions are DC isolated, which make it possible to bias diodes D_6 and D_7 independently. The states of PIN diodes are controlled by four DC pads V_{1+}, V_{5+}, V_{3-}, V_{4-}. Diode D_6 is forward biased by applying +5 V on DC pad V_1 and ground signal on V_{3-} pad. Diode D_7 is forward biased by applying +5 V on DC pad V_6 and ground signal on V_{4-} pad. When both diodes (D_6 and D_7) are in OFF state, modified cross slot obtains a structure which is symmetrical in x and y directions thereby produces linear polarization

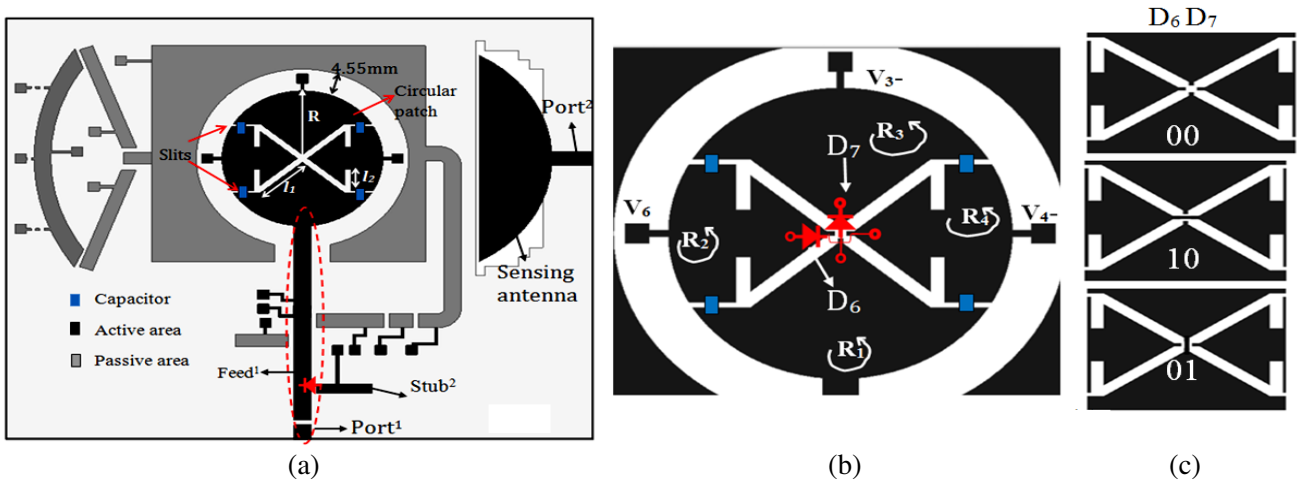

Figure 9. (a) Active portion of versatile antenna in polarization reconfigurable mode. (b) Diode biasing scheme. (c) Modified cross shaped slot under different diode conditions.

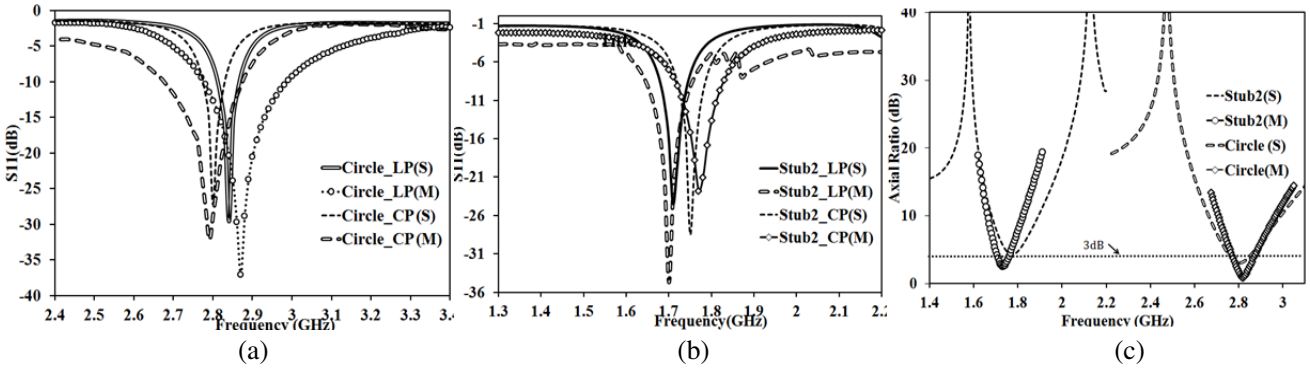

Figure 10. S_{11} vs. frequency for (a) case-A, (b) case-B, (c) axial ratio vs. frequency.

as shown in Fig. 9(c). When one of the diodes D_6 or D_7 is forward biased, cross-shape slot generates two equal and opposite modes thereby producing CP wave.

In this mode, antenna can switch its polarization state over two frequency bands, i.e., 2.84 GHz and 1.7 GHz. In the first case (Case-A for 2.84 GHz), only the circular patch is activated by controlling PIN diode D_1 state. In the second case (Case-B for 1.7 GHz), the circular antenna connected with stub^2 is activated by forward biasing the diode D_1 and D_3. The antenna's CP behavior is also analyzed under different stub combinations, but it is observed that in simulation antenna Axial Ratio (AR) is not good for stub^1 and stub^3, so they are not discussed here. Figs. 10(a)–(b) show the simulated and measured S_{11} vs. frequency for both cases. In Case-A, when diode D_1 is ON, and diodes D_6 and D_7 are OFF, the circular antenna radiates linear polarization at 2.84 GHz. The simulated resonant frequency is 2.84 GHz with RL = 30 dB whereas measured frequency is 2.87 GHz with RL = 37 dB. When either of the diodes D_6 and D_7 is ON, the antenna radiates CP signal. Due to the symmetry of the antenna structure, two PIN diodes (D_6 and D_7) have the same performances, so only the result for D_6 diode state is given here. The simulated resonant frequency 2.81 GHz has RL = 26 dB whereas measured resonant frequency 2.79 GHz has RL = 32 dB as shown in Fig. 10(a). In case-B, when diode D_1 and D_3 is forward biased, stub^2 tunes the resonate frequency of circular antenna at 1.7 GHz. In this case, antenna also shows CP behavior by controlling the PIN diode state D_6 and D_7. The simulated RL for linear polarization is 24 dB at 1.71 GHz whereas measured value of RL is 34 dB at 1.7 GHz as shown in Fig. 10(b). Similarly, simulated value of RL for circular polarization is 28 dB at 1.75 GHz whereas measured value of RL is 22 dB at 1.79 GHz. It is found that simulated and measured resonant frequencies are almost constant.

Axial ratios vs. frequency for both cases are given in Fig. 10(c). For Case-A, 3 dB AR bandwidth is 175 MHz whereas for Case B its value is 75 MHz.

3.3. Pattern Reconfiguration Mode

Figure 11 shows the active area of the proposed antenna when being operated in pattern reconfiguration mode. The rectangular patch which encloses the central patch at a distance of 4.55 mm away is active in this mode as direct RF signal is applied to it. In this mode, feed[2] is activated by forward biasing the diode D_4 and D_5 and keeping the D_1 in OFF state so that RF signal travels through $F_1S_3F_3$ structure. To reconfigure the radiation pattern diodes (D_8 and D_9) are forward biased by applying +5 V on V_7, V_8 pads and ground signal on V_{2-} pad. Now, three switchable shorting posts are designed at points 'B', 'C', 'D' on the parasitic arc. The active state of these shorting posts is controlled by using three PIN diodes namely D_{10}, D_{11}, D_{12}. As all the shorting points, i.e., 'B', 'C', 'D', are not directly attached to the active antenna, the resonant frequency does not shift. But shorting the parasitic arc results in shifts in the direction of radiation pattern because E field distribution in the antenna gets disturbed. The presence of short on the parasitic ring results in reformation of the electric field distribution leading to a shift of the main beam direction away from the short position. In all cases, change in the direction of the beam is defined by the combined effect of location of short at the parasitic arc and basic radiation pattern of the main patch in an ideal case. Generally, a null appears opposite to the position where the short is placed, but due to uneven distribution of the electric fields by the various components pattern can radiate in any direction with any shape.

Figures 11(b)–(c) show the observed S_{11} vs. frequency for this mode. Simulated and measured frequencies are nearly constant, and RL is better than 30 dB for all the cases. Simulated and measured radiation E plane patterns for all the cases are shown in Fig. 12. When no diode is forward biased,

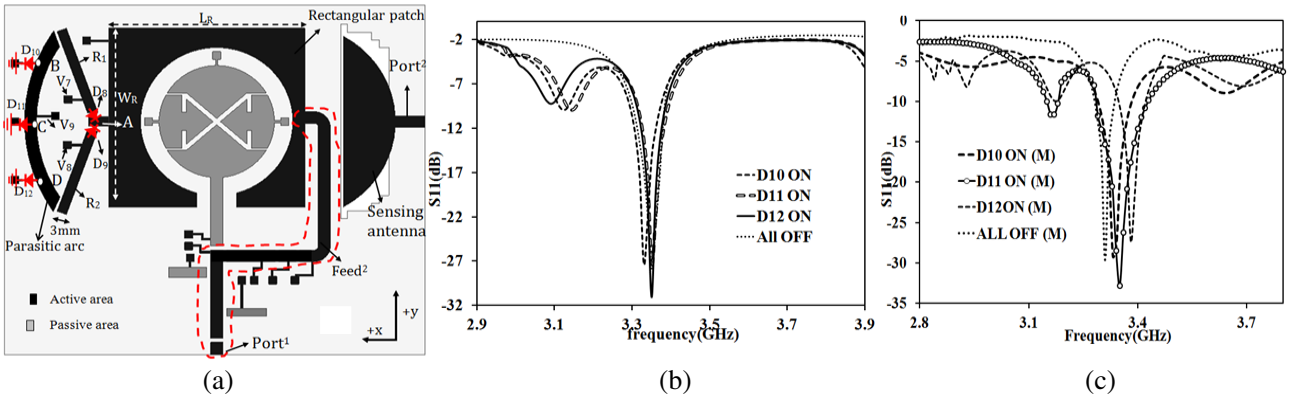

Figure 11. (a) Active area in pattern reconfiguration mode. (b) Simulated S parameter. (c) Measured S parameter.

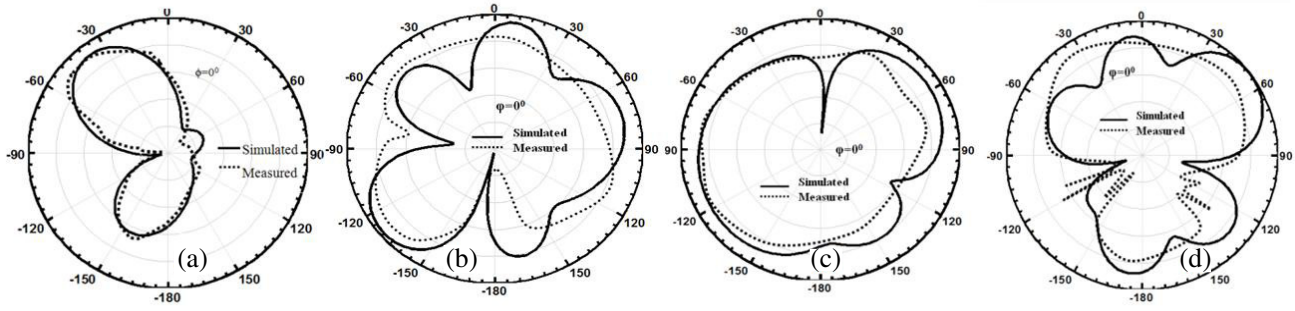

Figure 12. (a) E plane pattern for (a) all OFF, (b) D_{10} short, (c) D_{11} short, (d) D_{12} short.

the main patch radiates a bidirectional pattern as shown in Fig. 12(a). When D_{10} is forward biased, it shorts the arc at point B, and the observed pattern has a distorted omni-shape with maximum radiation towards $-130°$, shown in Fig. 12(b). When diode D_{11} is forward biased, it short the arc at point C, and the observed pattern has a distorted omni-shape as shown in Fig. 12(c). When diode D_{12} is forward biased, it shorts the arc at point D, and the observed pattern has a distorted dumbbell shape as shown in Fig. 12(d).

3.4. Spectrum Sensing Mode

For spectrum sensing mode, the hybrid antenna is excited by port[2], and simulated and measured UWB responses are shown in Fig. 13(a). The simulated and measured S_{11} are below 10 dB from 1 to 11 GHz. Fig. 13(b) shows that the observed pattern for gain is bidirectional in elevation plane and omnidirectional in azimuthal plane and greater than 4 dB for both planes.

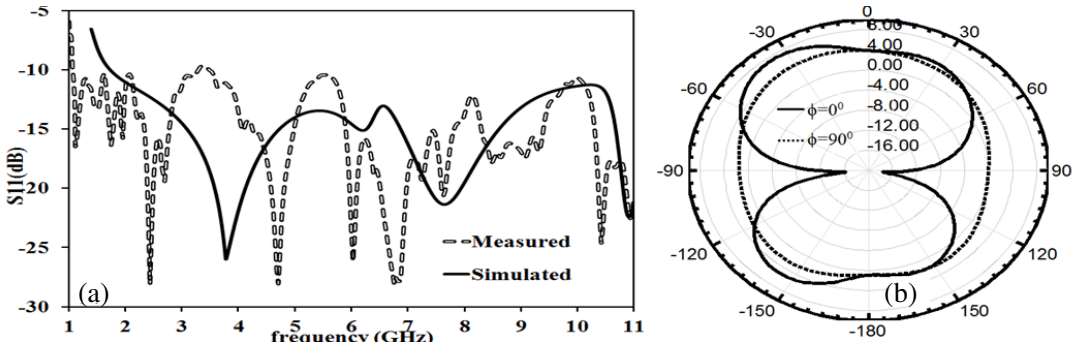

Figure 13. (a) Simulated and measured S_{11} parameter in UWB mode. (b) Gain (dB) at 5 GHz.

3.5. Bandwidth Reconfiguration Mode

In this mode, the antenna can reconfigure its operating bandwidth either in UWB mode or in any NB by switching the active port state. The proposed antenna will work for UWB mode if port[2] is activated, and it can switch its bandwidth over any one of the five NBs (case[1]–case[5]) by activating port[1].

In literature, a number of antennas are reported in which a separate sensing antenna is designed without degrading the overall performance [2–13]. In all these designs, the numbers of reconfigurable features are limited to one or two. Moreover, in some designs, extra matching circuitry is needed to make the design more flexible at the cost of increasing design complexity. Further-up-gradation of these antennas to increase the reconfiguration states is quite challenging because of the size constraint. This may compromise the goal of combining multiple reconfigurable functionalities in a single structure for CR systems. The proposed antenna is suitable for CR and superior to the reported designs as single antenna provides multiple reconfiguration features viz. spectrum sensing, frequency, bandwidth, polarization and radiation pattern. Moreover, the proposed antenna uses different ports for the active operation of individual antenna, so there is no need for port isolation as required in earlier reported designs. To the authors' best knowledge, there is no such a planar reconfigurable antenna with a combination of such features. However, the present structure is implemented only for the proof of concepts; antenna can be redesigned on interested frequency by designing the matching stubs for any commercial application. Furthermore, the inclusions of losses due to lumped element can be calculated by comparing simulated and measured realized gain patterns.

4. CONCLUSION

A versatile antenna capable of frequency, polarization, bandwidth and pattern reconfiguration in a single structure is proposed here. The functioning of each mode has been verified through measurement.

REFERENCES

1. Tawk, Y., M. Bkassiny, G. El-Howayek, S. K. Jayaweera, K. Avery, and C. G. Christodoulou, "Reconfigurable front-end antennas for cognitive radio applications," *IET Microwave Antennas Propagation*, Vol. 5, No. 8, 985–992, 2011.
2. Tawk, Y. and C. G. Christodoulou, "A new reconfigurable antenna design for cognitive radio," *IEEE Antennas and Wireless Propagation Letters*, Vol. 8, 1378–1381, 2009.
3. Sharma, S. and C. C. Tripathi, "Frequency reconfigurable U-slot antenna for SDR application," *Progress In Electromagnetics Research Letters*, Vol. 55, 129–136, 2015.
4. Sharma, S. and C. C. Tripathi, "Wideband to concurrent tri-band frequency reconfigurable microstrip patch antenna for wireless communication," *Int. Journal of Microwave and Wireless Tech.*, 1–10, 2016.
5. Tawk, Y., J. Costantine, K. Avery, and C. Christodoulou, "Implementation of a cognitive radio front-end using rotatable reconfigurable antennas," *IEEE Transactions on Antennas and Propagation*, Vol. 59, No. 5, 1773–1778, 2011.
6. Zheng, S. H., X. Y. Liu, and M. M. Tentzeris, "A novel optically controlled reconfigurable antenna for cognitive radio systems," *Antennas and Propagation Society International Symposium*, Jul. 6–11, 2014.
7. Tawk, Y., M. Bkassiny, G. El-Howayek1 S. K. Jayaweera, K. Avery, and C. G. Christodoulou, "Reconfigurable front-end antennas for cognitive radio applications," *IET Microwave Antennas Propagation*, Vol. 5, No. 8, 985–992, 2011.
8. Al-Husseini, M., Y. Tawk, C. G. Christodoulou, A. El-Hajj, and K. Y. Kabalan, "A reconfigurable cognitive radio antenna design," *IEEE AP-S International Symposium on Antennas and Propagation*, Toronto, Canada, Jul. 11–17, 2010.
9. Aboufoul, T., A. Alomainy, and C. Parini, "Reconfiguring UWB monopole antenna for cognitive radio applications using GaAs FET switches," *IEEE Antennas Wireless Propagation Letters*, Vol. 11, 392–394, Apr. 2012.
10. Ebrahimi, E., J. R. Kelly, and P. S. Hall, "Integrated wide-narrowband antenna for multi-standard radio," *IEEE Transactions on Antennas and Propagation*, Vol. 59, No. 7, 2628–2635, Jul. 2011.
11. Sharma, S. and C. C. Tripathi, "A wide spectrum sensing and frequency reconfigurable antenna for cognitive radio," *Progress In Electromagnetics Research C*, Vol. 67, 11–20, 2016.
12. Augustin, G. and T. A. Denidni, "An integrated ultra wideband/narrow band antenna in uniplanar configuration for cognitive radio systems," *IEEE Transactions on Antennas and Propagation*, Vol. 60, No. 11, 5479–5484, Nov. 2012.
13. Sharma, S. and C. C. Tripathi, "A versatile reconfigurable antenna for cognitive radio," *Asia Pacific Asia Pacific Microwave Conference, (APMC 2016)*, New Delhi, India, Dec. 5–9, 2016.